

APPROXIMATING THE TIME-FREQUENCY OUTPUT OF A DYNAMICAL SYSTEM FOR AN ARBITRARY NONSTATIONARY INPUT

Lorenzo Galleani

Politecnico di Torino, Corso Duca degli Abruzzi 24, 10129 Torino, Italy

ABSTRACT

We obtain the approximate analytic time-frequency spectrum of the output of a dynamical system when the input is an arbitrary finite-energy nonstationary signal. Our method is based on three steps. First, we transform the dynamical system to the time-frequency domain. Second, we approximate the time-frequency spectrum of the input as a sum of short duration sinusoids through a Fourier series expansion. Finally, we combine the time-frequency outputs corresponding to each individual short duration sinusoid, which are known in exact analytic form. An example shows that the proposed method requires a few terms only to obtain an approximate time-frequency output which is indistinguishable from the exact one. Furthermore, our method can clarify how dynamical systems process nonstationary signals. This processing mechanism is of fundamental interest since dynamical systems are a common model for real-world signals.

Index Terms— Time-frequency analysis, smoothed Wigner distribution, dynamical systems, nonstationary signals

1. INTRODUCTION

We consider the dynamical system defined by the differential equation [1]

$$a_n \frac{d^n x(t)}{dt^n} + \dots + a_1 \frac{dx(t)}{dt} + a_0 x(t) = f(t), \quad (1)$$

where $f(t)$ is the forcing term or input, $x(t)$ is the solution or output, and a_0, \dots, a_n are deterministic coefficients, with $a_n \neq 0$. The state of the system is the vector whose components are $x^{(k)}(t)$, for $k = 0, \dots, n-1$, where $x^{(k)}(t) = d^k x(t)/dt^k$ and $x^{(0)}(t) = x(t)$, whereas the law of evolution is the differential equation. We consider deterministic input signals $f(t)$. This dynamical system models a variety of real-world signals in electrical engineering [2], mechanical engineering [3], vibration of structures [4], thermodynamics [5], and pharmacokinetics [6]. It can also model nonlinear oscillations with small amplitude [7]. When the input $f(t)$ is nonstationary, the output $x(t)$ is nonstationary and its frequency content changes with time. Time-frequency analysis represents this time-varying spectrum in an effective way [8].

Even more effective is the direct time-frequency representation of (1) [9].

Since real-world signals are inherently nonstationary, understanding the nonstationary structure of the output is of fundamental interest. In [10] the exact analytic time-frequency spectrum of the output of (1) is derived for a series of common nonstationary input signals, namely, a delta function, a linear chirp, a causal sinusoid, and a short-duration sinusoid (a sinusoid with finite time support). The output is obtained first in the Wigner distribution representation [11], [12]

$$W_x(t, \omega) = \frac{1}{2\pi} \int_{-\infty}^{+\infty} x^*(t - \tau/2) x(t + \tau/2) e^{-i\tau\omega} d\tau, \quad (2)$$

and then in the smoothed Wigner domain

$$P_x(t, \omega) = \int_{-\infty}^{+\infty} w(t - t') W_x(t', \omega) dt', \quad (3)$$

where the smoothing window $w(t)$ is a Hann, Hamming, or rectangular window. This smoothed Wigner distribution provides an effective reduction of the interference terms of the output Wigner representations [10]. The obtained time-frequency outputs are exact analytic results, since no approximation method is used.

When $f(t)$ is an arbitrary nonstationary signal, though, the analytic time-frequency output cannot be computed exactly. In [13] an approximation method for signals filtered by linear time-invariant (LTI) systems is discussed. The method approximates the Wigner distribution of the output of the LTI system by using its transfer function and the Wigner distribution of the input. In [14] the Wigner distribution of the output for the dynamical system (1) is approximated for the class of polynomial chirp signals. Other approximation techniques for the Wigner distribution are discussed in [15], [16]. In this article, we instead propose an approximation method for the smoothed Wigner output of (1) when the input is an arbitrary finite-energy nonstationary signal. The approximation is obtained by expanding the time-frequency input in a sum of short duration sinusoids through a Fourier series expansion. The time-frequency output is obtained by adding up the time-frequency outputs corresponding to the individual short duration sinusoids at the input, which are derived in exactly analytic form in [10]. The quality of the approximation is controlled by the number of terms in the Fourier series.

We show an example of a system with two resonances whose input signal is a sinusoid with Gaussian amplitude. By using five terms only in the Fourier expansion (plus the DC component) we derive an approximate time-frequency output which is indistinguishable from the exact one, obtained by numerical simulations. The effectiveness of our approximation method is justified by the fact that, for a wide variety of nonstationary real-world signals, the time-frequency spectrum is made by concentrated and relatively smooth functions, commonly referred to as components. Approximating concentrated and smooth functions is, in general, easier than approximating the signal in the disjoint time and frequency domains, particularly with the Fourier series decomposition.

Our method can clarify the time-frequency structure of nonstationary signals. The availability of the analytic time-frequency output reveals in fact the spectral mechanisms involved in the processing of nonstationary signals. This insight can hardly be obtained with numerical techniques only. Furthermore, we believe that our method can foster the development of improved system design and identification methods that operate directly in the time-frequency domain.

The article is organized as follows. In Sect. 2 we obtain the approximation method and in Sect. 3 we discuss an analytic example.

2. APPROXIMATION METHOD

We start by factoring (1)

$$a_n \prod_{m=1}^n (D - \lambda_m) x(t) = f(t), \quad (4)$$

where $D = \frac{d}{dt}$, $\lambda_1, \dots, \lambda_n$ are the poles of the dynamical system in time, and we define $f(t)$ and $x(t)$ on the entire time axis $-\infty < t < +\infty$. The Wigner representation of this system is [17]

$$\frac{|a_n|^2}{4^n} \prod_{m=1}^n (\partial_t - p_m(\omega)) (\partial_t - p_m^*(\omega)) W_x(t, \omega) = W_f(t, \omega), \quad (5)$$

where $\partial_t = \frac{\partial}{\partial t}$, the quantities $p_m(\omega) = 2\alpha_m + 2i(\beta_m - \omega)$ are the time-frequency poles, and α_m, β_m are the real and imaginary parts of the generic pole λ_m , respectively. Equation (5) is a time-frequency dynamical system, whose input $W_f(t, \omega)$ is the Wigner distribution of the input $f(t)$, and whose output $W_x(t, \omega)$ is the Wigner distribution of the output $x(t)$. We note that, although the Wigner distribution is nonlinear, the time-frequency dynamical system is still linear with respect to the Wigner input $W_f(t, \omega)$. Moreover, the coefficients are a function of ω only and there is no derivative with respect to ω , therefore we can write the Wigner output as [18]

$$W_x(t, \omega) = \int_{-\infty}^{+\infty} W_h(t - t', \omega) W_f(t', \omega) dt', \quad (6)$$

where $W_h(t, \omega)$ is the impulse response of the time-frequency system. We rewrite this result as

$$W_x(t, \omega) = \mathcal{L}[W_f(t, \omega)], \quad (7)$$

where \mathcal{L} is the linear operator representing convolution.

The approximate Wigner input is now obtained via the Fourier series expansion

$$\begin{aligned} \tilde{W}_f(t, \omega) &= A_0(\omega) + \sum_{n=1}^N A_n(\omega) \cos\left(\frac{2\pi}{T} nt\right) \\ &\quad + \sum_{n=1}^N B_n(\omega) \sin\left(\frac{2\pi}{T} nt\right), \end{aligned} \quad (8)$$

where $0 < t < T$, and

$$A_0(\omega) = \frac{1}{T} \int_0^T W_f(t, \omega) dt, \quad (9)$$

$$A_n(\omega) = \frac{2}{T} \int_0^T W_f(t, \omega) \cos\left(\frac{2\pi}{T} nt\right) dt, \quad (10)$$

$$B_n(\omega) = \frac{2}{T} \int_0^T W_f(t, \omega) \sin\left(\frac{2\pi}{T} nt\right) dt. \quad (11)$$

The time instant T must be chosen so that most of the Wigner input $W_f(t, \omega)$ is concentrated in $0 < t < T$. We note that, for a finite-energy signal $g(t)$, it is [8]

$$\int_{-\infty}^{+\infty} |g(t)|^2 dt = \iint_{-\infty}^{+\infty} W_g(t, \omega) dt d\omega < +\infty, \quad (12)$$

and hence for an arbitrarily small $\gamma > 0$ we can always find two time values t_1, t_2 such that

$$\left| \int_{-\infty}^{t_1} \int_{-\infty}^{+\infty} W_g(t, \omega) dt d\omega + \int_{t_2}^{+\infty} \int_{-\infty}^{+\infty} W_g(t, \omega) dt d\omega \right| \leq \gamma. \quad (13)$$

We point out that $W_g(t, \omega)$ is real [8] and, in general, locally negative. The double integrals in (13), though, are positive, since

$$\int_{-\infty}^{+\infty} W_g(t, \omega) d\omega = |g(t)|^2. \quad (14)$$

By setting $f(t) = g(t + t_1)$ and $T = t_2 - t_1$ we can hence state that $W_f(t, \omega)$ has most of its information in $0 < t < T$. In a future publication we will show how to extend our method to a broader class of signals.

We rewrite (8) as

$$\begin{aligned} \tilde{W}_f(t, \omega) &= A_0(\omega) P_T(t - T/2) \\ &\quad + \sum_{n=1}^N A_n(\omega) P_T(t - T/2) \cos(\omega_n t) \\ &\quad + \sum_{n=1}^N B_n(\omega) P_T(t - T/2) \sin(\omega_n t), \end{aligned} \quad (15)$$

where $\omega_n = 2\pi n/T$ and $P_T(t)$ is the rectangular window defined as $P_T(t) = 1$ for $|t| \leq T/2$, and $P_T(t) = 0$ for $|t| > T/2$. By using the notation of [10], we have

$$\begin{aligned}\tilde{W}_f(t, \omega) &= A_0(\omega)F_{\text{SDC}}(t, \omega; T) \\ &+ \sum_{n=1}^N A_n(\omega)F_{\text{SDS}}(t, \omega; \omega_n, \pi/2, T) \\ &+ \sum_{n=1}^N B_n(\omega)F_{\text{SDS}}(t, \omega; \omega_n, 0, T),\end{aligned}\quad (16)$$

where F_{SDC} , F_{SDS} are the generalized inputs corresponding to the short duration constant (SDC) and short duration sinusoid (SDS), defined as

$$\begin{aligned}F_{\text{SDC}}(t, \omega; T) &= P_T(t - T/2), \\ F_{\text{SDS}}(t, \omega; \omega_n, \varphi, T) &= P_T(t - T/2) \sin(\omega_n t + \varphi).\end{aligned}\quad (17)$$

The term generalized inputs indicates that both F_{SDC} and F_{SDS} do not represent proper Wigner distributions. From (7) it is

$$\tilde{W}_x(t, \omega) = \mathcal{L}[\tilde{W}_f(t, \omega)].\quad (19)$$

We replace $\tilde{W}_f(t, \omega)$ and we use the linearity of \mathcal{L} , obtaining

$$\begin{aligned}\tilde{W}_x(t, \omega) &= A_0(\omega)\mathcal{L}[F_{\text{SDC}}(t, \omega; T)] \\ &+ \sum_{n=1}^N A_n(\omega)\mathcal{L}[F_{\text{SDS}}(t, \omega; \omega_n, \pi/2, T)] \\ &+ \sum_{n=1}^N B_n(\omega)\mathcal{L}[F_{\text{SDS}}(t, \omega; \omega_n, 0, T)].\end{aligned}\quad (20)$$

It is

$$\begin{aligned}\tilde{W}_x(t, \omega) &= A_0(\omega)X_{\text{SDC}}(t, \omega; T) \\ &+ \sum_{n=1}^N A_n(\omega)X_{\text{SDS}}(t, \omega; \omega_n, \pi/2, T) \\ &+ \sum_{n=1}^N B_n(\omega)X_{\text{SDS}}(t, \omega; \omega_n, 0, T),\end{aligned}\quad (21)$$

where X_{SDC} , X_{SDS} are the generalized outputs, derived in [10] by solving (5) when the forcing terms are the generalized inputs F_{SDC} , F_{SDS} . The generalized input/output technique simplifies dramatically the analytic calculation of the time-frequency outputs. We do not report the explicit generalized outputs here for conciseness.

Finally, from (3), the approximate smoothed Wigner output $\tilde{P}_x(t, \omega)$ is given by

$$\tilde{P}_x(t, \omega) = \int_{-\infty}^{+\infty} w(t - t')\tilde{W}_x(t', \omega)dt'.\quad (22)$$

Since convolution is a linear operation, we can write

$$\begin{aligned}\tilde{P}_x(t, \omega) &= A_0(\omega)\bar{X}_{\text{SDC}}(t, \omega; T) \\ &+ \sum_{n=1}^N A_n(\omega)\bar{X}_{\text{SDS}}(t, \omega; \omega_n, \pi/2, T) \\ &+ \sum_{n=1}^N B_n(\omega)\bar{X}_{\text{SDS}}(t, \omega; \omega_n, 0, T),\end{aligned}\quad (23)$$

where \bar{X}_{SDC} , \bar{X}_{SDS} are the smoothed generalized outputs derived in [10] by convolving the generalized outputs with the smoothing window $w(t)$. We do not report the explicit smoothed generalized outputs here for brevity.

We point out that, for finite-energy input signals, we can always increase the time interval T and the number of terms N in the expansion to reach the desired approximation quality. A high quality approximation with a small number of terms N , though, can be achieved with input signals made by concentrated components. This class of signals is extremely common in physical systems.

3. EXAMPLE

We consider a system of order $n = 4$ with two resonances, defined by the poles (we use dimensionless quantities for simplicity)

$$\begin{aligned}\lambda_1 &= -2.5 + 6\pi i, & \lambda_2 &= \lambda_1^*, \\ \lambda_3 &= -0.8 + 15\pi i, & \lambda_4 &= \lambda_3^*.\end{aligned}\quad (24)$$

We take a sinusoid with Gaussian amplitude as the input,

$$f(t) = e^{-(t-T/2)^2/(4\sigma^2) + i\omega_0(t-T/2)},\quad (25)$$

with $T = 4$ and $\sigma = T/10 = .4$. The peak of the Gaussian amplitude is at $t = T/2$. The Wigner distribution of this input signal is the Gaussian function [8]

$$W_f(t, \omega) = \frac{\sigma}{\sqrt{\pi/2}} e^{-(t-T/2)^2/(2\sigma^2) - 2\sigma^2(\omega - \omega_0)^2}.\quad (26)$$

Since $W_f(t, \omega)$ is symmetric with respect to $t = T/2$, the coefficients B_n in (11) are all zero, and (23) becomes

$$\begin{aligned}\tilde{P}_x(t, \omega) &= A_0(\omega)\bar{X}_{\text{SDC}}(t, \omega; T) \\ &+ \sum_{n=1}^N A_n(\omega)\bar{X}_{\text{SDS}}(t, \omega; \omega_n, \pi/2, T),\end{aligned}\quad (27)$$

for $0 < t < T$. By using the properties of the Fourier series, it is

$$A_0 = 2\frac{\sigma^2}{T} e^{-2\sigma^2(\omega - \omega_0)^2},\quad (28)$$

$$A_n = 4(-1)^n \frac{\sigma^2}{T} e^{-2\sigma^2(\omega - \omega_0)^2} e^{-2\pi^2\sigma^2 n^2/T^2}.\quad (29)$$

We note that these coefficients are actually computed for the periodic function $G_f(t, \omega) = \sum_{k=-\infty}^{+\infty} W_f(t - kT, \omega)$. Since

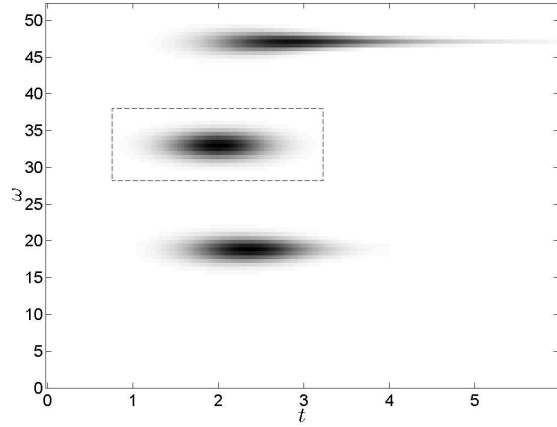


Fig. 1. Wigner input and approximate analytic smoothed Wigner outputs. The plot shows the Wigner input $W_f(t, \omega)$ (dashed box), obtained when $\omega_0 = 10.5\pi$ and displayed as a reference, as well as the approximate analytic smoothed Wigner outputs obtained when $\omega_0 = 6\pi$ and $\omega_0 = 15\pi$, corresponding to the two resonant frequencies of the system. The response for the higher resonant frequency lasts longer due to the smaller damping of this resonance. The approximate analytic outputs are obtained with $N = 5$ terms (plus a constant).

$T \gg \sigma$ it is $G_f(t, \omega) \approx W_f(t, \omega)$ for $0 < t < T$. Replacing the Fourier coefficients in (27) gives

$$\begin{aligned} \tilde{P}_x(t, \omega) = & 2 \frac{\sigma^2}{T} e^{-2\sigma^2(\omega - \omega_0)^2} \bar{X}_{\text{SDC}}(t, \omega; T) \\ & + \sum_{n=1}^N 4(-1)^n \frac{\sigma^2}{T} e^{-2\sigma^2(\omega - \omega_0)^2} \\ & \times e^{-2\pi^2 \sigma^2 n^2 / T^2} \bar{X}_{\text{SDS}}(t, \omega; \omega_n, \pi/2, T), \end{aligned} \quad (30)$$

which is the desired approximate time-frequency output.

In Fig. 1 we show this result by superimposing three time-frequency distributions. First, in the dashed box we show the input Wigner $W_f(t, \omega)$ computed for $\omega_0 = 10.5\pi$. This Wigner input is displayed as a reference to understand the shape of the resulting time-frequency outputs. Second, we show the approximate smoothed Wigner output $\tilde{P}_x(t, \omega)$ computed when the frequency of the input sinusoid is $\omega_0 = 6\pi$, which corresponds to the lower resonant frequency. We see that the time-frequency output is centered about the resonant frequency, and its peak is delayed with respect to the peak of the input Wigner $W_f(t, \omega)$ due to the processing time required by the system. The approximation is obtained with $N = 5$. Third, we show the approximate smoothed Wigner output $\tilde{P}_x(t, \omega)$ when $\omega_0 = 15\pi$, which corresponds to the higher resonant frequency. We see that this time-frequency output is further delayed, with respect to the Wigner input $W_f(t, \omega)$, than the output at the lower resonant frequency. The increase in the delay is due to the smaller

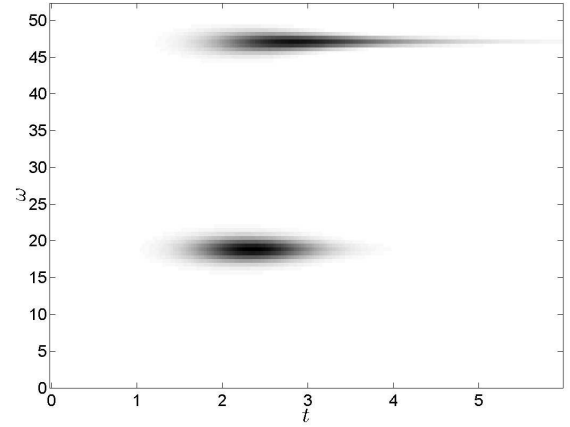


Fig. 2. Smoothed Wigner outputs obtained by numerical simulations. The smoothed Wigner outputs are practically indistinguishable from the approximate analytic versions shown in Fig. 1.

damping of this resonance, which also causes the output to last longer in time. Also this approximation is obtained with $N = 5$.

In Fig. 2 we show the same time-frequency distributions of Fig. 1 obtained by numerical computations. We see that the approximate smoothed Wigner outputs and the numerical ones are practically indistinguishable. The percent error of the approximation, defined as

$$\epsilon = 100 \frac{\int_{-\infty}^{+\infty} \int_{-\infty}^{+\infty} (\tilde{P}_x(t, \omega) - P_x^{\text{Num}}(t, \omega)) dt d\omega}{\int_{-\infty}^{+\infty} \int_{-\infty}^{+\infty} P_x^{\text{Num}}(t, \omega) dt d\omega}, \quad (31)$$

where $P_x^{\text{Num}}(t, \omega)$ is the smoothed Wigner output obtained by numerical methods, is in fact smaller than 0.3% for both resonances.

4. CONCLUSIONS

We have developed a method to evaluate the approximate analytic time-frequency output of a dynamical system whose input is an arbitrary finite-energy nonstationary signal. The method is based on a Fourier series approximation of the time-frequency input signal. The quality of the approximation can be controlled by changing the number of terms in the Fourier expansion, although an example shows that a few terms only produce an approximation of the time-frequency output that is indistinguishable from the exact one. The approximate analytic time-frequency output can clarify the spectral mechanism involved in the generation of nonstationary signals. This result can be hardly achieved with numerical methods only.

5. REFERENCES

- [1] A. Katok and B. Hasselblatt, *Introduction to the modern theory of dynamical systems*, Cambridge University Press, 1996.
- [2] L. O. Chua, C. A. Desoer, and E. S. Kuh, *Linear and Nonlinear Circuits*, McGraw-Hill, 1987.
- [3] M. L. James, G. M. Smith, J. C. Wolford, and P. W. Whaley, *Vibration of Mechanical and Structural Systems*, HarperCollins College Publishers, 1994.
- [4] R. W. Clough, *Dynamics of structures*, Mc-Graw Hill, 1993.
- [5] J. T. Hsu and L. Vu-Quoc, "A rational formulation of thermal circuit models for electrothermal simulation – Part I: Finite element method," *IEEE Trans. Circ. Sys. I*, vol. 43, no. 9, 1996.
- [6] D. W. A. Bourne, "Pharmacokinetics," in G. S. Banker and C. Rhodes (Eds.), *Modern pharmaceuticals*, Informa Healthcare, 2002.
- [7] A. H. Nayfeh and D. T. Mook, *Nonlinear Oscillations*, Wiley-VCH, 1995.
- [8] L. Cohen, *Time-Frequency Analysis*, Prentice-Hall, 1995.
- [9] L. Galleani and L. Cohen, "Direct Time-Frequency Characterization of Linear Systems Governed by Differential Equations," *IEEE Signal Processing Letters*, vol. 11, pp. 721-724, 2004.
- [10] L. Galleani, "Response of Dynamical Systems to Non-stationary Inputs," *IEEE Trans. Sig. Process.*, vol. 60, no. 11, pp. 5775-5786, 2012.
- [11] E. P. Wigner, "On the quantum correction for thermodynamic equilibrium," *Physical Review*, vol. 40, pp. 749–759, 1932.
- [12] W. Mecklenbrauker and F. Hlawatsch (Eds.), *The Wigner distribution: theory and applications in signal processing*, Elsevier, 1997.
- [13] P. Loughlin, "Time-Varying Spectral Approximation of Filtered Signals," *IEEE Signal Processing Letters*, vol. 13, no. 10, pp. 604-607, 2006.
- [14] L. Galleani and L. Cohen, "Approximation of the Wigner Distribution for Dynamical Systems Governed by Differential Equations," *EURASIP Journal on Applied Signal Processing*, vol. 2002, no. 1, pp. 67-72, 2002.
- [15] A. G. Athanassoulis, N. J. Mauser, and T. Paul, "Coarse-scale representations and smoothed Wigner transforms," *Journal de mathematiques pures et appliquees*, vol. 91, no. 3, pp. 296-338, 2009.
- [16] N. Snider, "Semiclassical phase space representation of the density matrix," *J. Chem. Phys.*, vol. 69, no. 8, pp. 3545-3547, 1978.
- [17] L. Galleani, "The transient spectrum of a random system," *IEEE Trans. Sig. Process.*, vol. 58, no. 10, pp. 5106-5117, 2010.
- [18] T. A. C. M. Claasen and W. F. G. Mecklenbrauker, "The Wigner Distribution - a tool for time-frequency signal analysis, Part I: continuous-time signals," *Philips J. Res.*, vol. 35, pp. 217-250, 1980.